SIMULATION OF THE SUPERCRITICAL FLOW AROUND A CIRCULAR CYLINDER USING HYBRID MODELS

F.Miralles[1], S.Wornom[1], B.Koobus[1], A.Dervieux[2,3]

[1] **IMAG, université de Montpellier, France,**
[2] **Société LEMMA, Sophia-Antipolis, France**
[3] **INRIA Sophia-Antipolis, France**

33rd Nordic Seminar on Computational Mechanics, Jönköping, 25-26 november, 2021

- Why high Reynolds number ?

Figure – Helicopter blades application, wind turbines

- Why cylinder ?

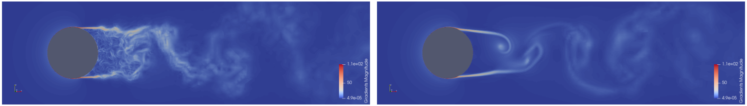

Figure – Flow Past a Cylinder at Re=1M, vorticty field.

Modeling of turbulent flow : RANS description

- Compressible Averaged Navier Stokes Equation :

$$\frac{\partial W_h}{\partial t} + \nabla \cdot F_c(W_h) - \nabla \cdot F_d(W_h) = \tau(W_h) \qquad (1)$$

- RANS $k - \varepsilon$ Goldberg closure term :

$$\tau^{RANS}(W_h) = \left(\overbrace{0}^{\rho}, \overbrace{\mathbf{0}}^{\rho\mathbf{u}}, \overbrace{0}^{\rho E}, \overbrace{\tau : \nabla\mathbf{u} - \rho\epsilon}^{\rho k}, \overbrace{(C_1 \tau : \nabla\mathbf{u} - C_2 \rho\epsilon + E) T^{-1}}^{\rho\epsilon} \right)$$

- DDES closure term $\rho\epsilon$ is replaced by $\rho\frac{k^{3/2}}{\mathfrak{l}_{ddes}}$ where :

$$\mathfrak{l}_{ddes} = \frac{k^{\frac{3}{2}}}{\epsilon} - f_{ddes} \max\left(0, \frac{k^{\frac{3}{2}}}{\epsilon} - 0.65\Delta\right), \quad \begin{aligned} f_{ddes} &= 1 - \tanh((8r_d)^3), \\ r_d &= \frac{\nu_t + \nu}{\kappa^2 y^2 \max(\sqrt{\nabla\mathbf{u} : \nabla\mathbf{u}}, 10^{-10})} \end{aligned}$$

Dynamic VMS description

- VMS formulation

$$\left(\frac{\partial W_h}{\partial t},\chi_i\right)+(\nabla\cdot F_c(W_h),\chi_i)=(\nabla\cdot F_d(W_h),\phi_i)+\left(\tau^{DVMS}(W_h),\phi_i'\right). \qquad (2)$$

- VMS closure term with dynamics coefficients $\mathcal{C}_{model}=\mathcal{C}_{model}(\mathbf{x},t)$ and $Pr_t=Pr_t(\mathbf{x},t)$

$$\left(\tau^{DVMS}(W_h),\phi_i'\right)=\left(0,\mathbf{M}_S(W_h,\phi_h'),M_H(W_h,\phi_h'),0,0\right)$$

where :

$$\begin{aligned}\mathbf{M}_S(W_h,\phi_i') &= \sum_{T\in\Omega_h}\int_T \underbrace{\overline{\rho}(C_S\Delta)^2|S|}_{\mu_{sgs}}\mathcal{D}(S)\nabla\phi_i'd\mathbf{x},\\ M_H(W_h,\phi_i') &= \sum_{T\in\Omega_h}\int_T \frac{C_p}{Pr_t}\underbrace{\overline{\rho}(C_S\Delta)^2|S|}_{\mu_{sgs}}\nabla T'\cdot\nabla\phi_i'd\mathbf{x}\end{aligned}\quad,\qquad \Delta=\left(\int_T d\mathbf{x}\right)^{1/3}$$

and $\phi_h'=\phi_h-\overline{\phi_h}$ where $\overline{\phi_h}$ is computed from macro cells.

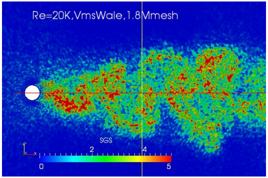

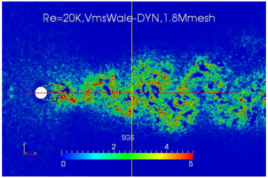

- Hybrid description with finite volume/ finite element method

$$\left(\frac{\partial W_h}{\partial t}, \chi_i\right) + (\nabla \cdot F_c(W_h), \chi_i) = (\nabla \cdot F_d(W_h), \phi_i) \tag{3}$$

$$+ \theta \left(\tau^C(W_h), \phi_i\right) + (1-\theta)\left(\tau^{DVMS}(W_h'), \phi_i'\right). \tag{4}$$

$\tau^C \in \{\tau^{RANS}, \tau^{DDES}\}$

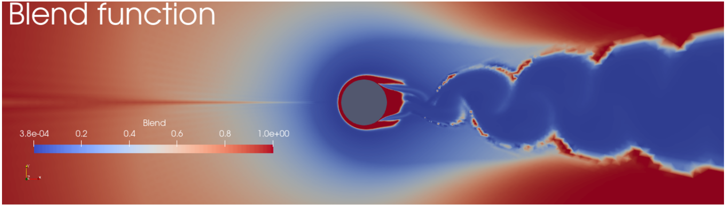

Figure – Hybrid RANS blending surface.

Set up

- Model used : DDES, RANS/DVMS, DDES/DVMS with :
  - Blending : $\theta = 1 - f_d \times (1 - \overline{\theta})$; $\quad \overline{\theta} = \tanh\left(\left(\frac{\Delta}{k^{3/2}}\varepsilon\right)^2\right)$,
  - Subgrid model for VMS : WALE, Smagorinsky
  - Closure model for RANS $k - \varepsilon$ of Goldberg.
- Simulation set up :
  - Mach number : 0.1 (subsonic flow)
  - reference pressure : 101300 $[\mathrm{N/m^2}]$
  - density : 1.225 $[\mathrm{kg/m^3}]$
  - Integration to the wall or Reichardt wall law :

$$U^+ = \frac{1}{\kappa}\ln\left(1 + \kappa y^+\right) + 7.8\left[1 - \exp\left(\frac{-y^+}{11}\right) - \frac{-y^+}{11}\exp\left(\frac{-y^+}{3}\right)\right]$$

  - The mesh is radial with minimal mesh size is such that $y_w^+ = 1 \Leftrightarrow \delta = 2 \times 10^{-5}$.

Name	Mesh size	y_w^+	y_m^+	$\overline{C}_d$	C_l'	$-\overline{C}_{pb}$	L_r	$\overline{\theta}$
Present simulation								
URANS $k-\varepsilon$	4.8M	1	0	0.50	0.24	0.61	0.77	109
DDES $k-\varepsilon$ Goldberg WL	4.8M	20	100	0.20	0.04	0.22	0.87	138
DDES $k-\varepsilon$ Goldberg WL	4.8M	20	25	0.40	0.05	0.56	1.46	113
DDES $k-\varepsilon$ Goldberg ITW	4.8M	1	0	0.50	0.07	0.54	1.22	103
DVMS								
cubic Smagorinsky ITW	4.8M	20	0	0.49	0.17	0.42	0.71	92
DDES/ DVMS								
k - ε / cubic WL Smagorinsky	4.8M	20	100	0.20	0.02	0.22	0.82	135
k - ε / cubic WALE WL	4.8M	1	100	0.20	0.02	0.26	0.80	132
k - ε / cubic WALE ITW	4.8M	1	0	0.49	0.06	0.60	1.56	104
RANS / DVMS								
k - ε / cubic Smagorinsky WL	4.8M	20	100	0.24	0.05	0.22	0.62	133
k - ε / cubic Smagorinsky WL	4.8M	1	100	0.25	0.09	0.25	0.64	132
k - ε / cubic WALE WL	4.8M	1	100	0.26	0.11	0.22	0.65	134
k - ε / cubic WALE ITW	4.8M	1	0	0.48	0.11	0.55	1.14	109
Other simulations								
RANS[1] Catalano [1] WL	2.3M	-	-	0.39	-	0.33		
LES Catalano [1] WL	2.3M	-	-	0.31	-	0.32		
LES Kim [3] WL	6.8M	-	-	0.27	0.12	0.28	-	108
Expériences								
Shih et *al* [5]				0.24	-	0.33		
Schewe [4]				0.22	-	-		
Szechenyi [6]				0.25	-	0.32		
Gölling [9]							-	130
Zdravkovich [8]				0.2-0.4	0.1-0.15	0.2-0.34		

Table – Bulk coefficient of the flow around a circular cylinder at Reynolds number 1M, $\overline{C}_d$ holds for the mean drag coefficient, C_l' is the root mean square of lift time fluctuation, $\overline{C}_{p_b}$ is the pressure coefficient at cylinder basis, L_r is the mean recirculation lenght, $\overline{\theta}$ is the mean separation angle.

---

[1] Steady RANS computation

- Pressure coefficient

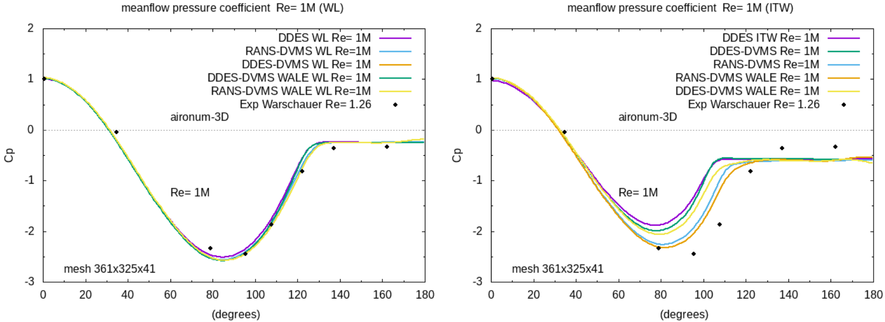

Figure – Distribution of mean pressure as a function of polar angle. Comparison with $y_w^+ = 20$ with Smagorinsky and $y+_w = 1$ with WALE. Wall law on the left and integration to the wall on the right.

- Integration to the Wall Q-criteria

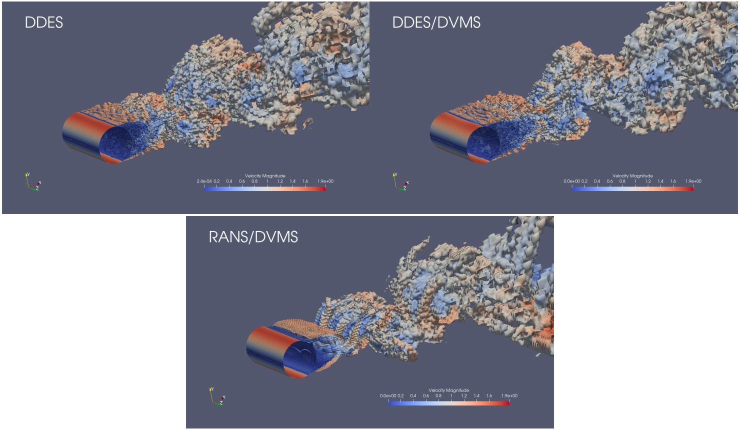

Figure – Q-criteria contour using velocity color scale.

Conclusion and perspective

- Bulks coefficients are accurately predicts with RANS/DVMS model,
- RANS/DVMS approach with WALE model gives the best results,
- Bulk coefficients are closer to experimental data for WL,
- Drag coefficients are overestimated for ITW,
- Implement a transition prediction model in order to more accurately compute transitional boundary layers .
- $k-\omega$ SST model, $k-R$ model

Annexe

Velocity profile

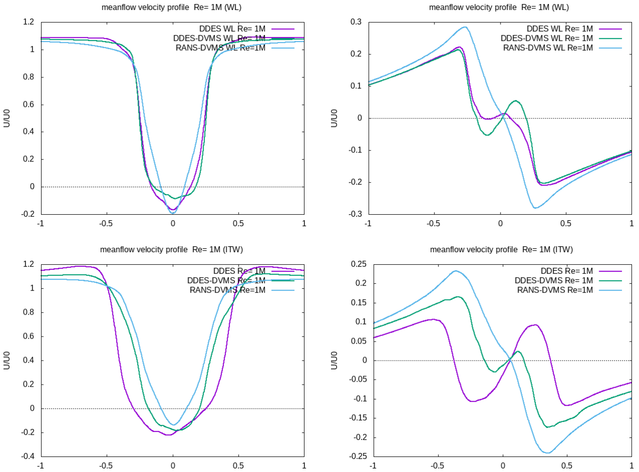

Figure – On the left longitudinal velocity profile at $x/D = 1$, and on right the transverse velocity.

P. Catalano, M.Wang, G. Iaccarino and P. Moin. Numerical simulation of the flow around a circular cylinder at High Reynolds numbers. *International Journal of Heat and Fluid Flow*, 24 :463-469, 2003.

Y. Ono and T. Tamura. LES of flows around a circular cylinder in the critical Reynolds number region. *Proceedings of BBAA VI International Colloquium on : Bluff Bodies Aerodynamics and Applications*, Milano, Italy, July 20-24 2008.

S.E. Kim and L.S. Mohan. Prediction of unsteady loading on a circular cylinder in high Reynolds number flows using large eddy simulation. *Proceedings of OMAE 2005 : 24th International Conference on Offshore Mechanics and Artic Engin.*

G. Schewe. On the force fluctuations acting on a circular cylinder in crossflow from subcritical up to transcritical Reynolds numbers. *Journal of Fluid Mechanics*, 133 :265-285, 1983.

W.C. L. Shih, C.Wang, D. Coles and A. Roshko. Experiments on Flow past rough circular cylinders at large Reynolds numbers. *Journal of Wind Engeneering and Industrial Aerodynamics*, 49 :351-368, 1993.

E. Szechenyi. Supercritical reynolds number simulation for two-dimensional flow over circular cylinders. *Journal of Fluid Mechanics*, 70 :529-542, 1975.

O. Guven, C. Farell, and V.C. Patel. Surface-roughness effects on the mean flow past circular cylinders. *Journal of Fluid Mechanics*, 98(4) :673-701, 1980.

M.M. Zdravkovich. Flow around circular cylinders Vol 1 : Fundamentals. *Oxford University Press*, 1997.

B. Gölling. Experimental Investigations of Separating Boundary-Layer Flow from Circular Cylinder at Reynolds Numbers from 105 up to 107 ; three-dimensional vortex flow of a circular cylinder. *G.E.A. Meier and K.R. Sreenivasan, editors, Proceedings of IUTAM Symposium on One Hundred Years of Boundary Layer Research*, pages 455-462, The Netherlands, 2006. Springer.